Ocean Dynamics (2011) 61:1927–1935
DOI 10.1007/s10236-011-0447-y

Surf zone characterization from Unmanned Aerial Vehicle imagery

Rob A. Holman · K. Todd Holland · Dave M. Lalejini · Steven D. Spansel

Received: 23 January 2011 / Accepted: 27 May 2011 / Published online: 14 June 2011
© Springer-Verlag (outside the USA) 2011

Abstract We investigate the issues and methods for estimating nearshore bathymetry based on wave celerity measurements obtained using time series imagery from small unmanned aircraft systems (SUAS). In contrast to time series imagery from fixed cameras or from larger aircraft, SUAS data are usually short, gappy in time, and unsteady in aim in high frequency ways that are not reflected by the filtered navigation metadata. These issues were first investigated using fixed camera proxy data that have been intentionally degraded to mimic these problems. It has been found that records as short as 50 s or less can yield good bathymetry results. Gaps in records associated with inadvertent look-away during unsteady flight would normally prevent use of the required standard Fast Fourier Transform methods. However, we found that a full Fourier Transform could be implemented on the remaining valid record segments and was effective if at least 50% of total record length remained intact. Errors in image geo-navigation were stabilized based on fixed ground fiducials within a required land portion of the image. The elements of a future method that could remove this requirement were then outlined. Two test SUAS data runs were analyzed and compared to survey ground truth data. A 54-s data run at Eglin Air Force Base on the Gulf of Mexico yielded a good bathymetry product that compared well with survey data (standard deviation of 0.51 m in depths ranging from 0 to 4 m). A shorter (30.5 s) record from Silver Strand Beach (near Coronado) on the US west coast provided a good approximation of the surveyed bathymetry but was excessively deep offshore and had larger errors (1.19 m for true depths ranging from 0 to 6 m), consistent with the short record length. Seventy-three percent of the bathymetry estimates lay within 1 m of the truth for most of the nearshore.

Keywords Bathymetry · Unmanned systems · Nearshore processes · Littoral

Responsible Editor: Michel Rixen

This article is part of the Topical Collection on *Maritime Rapid Environmental Assessment*

R. A. Holman · K. T. Holland · D. M. Lalejini · S. D. Spansel
Code 7440, Naval Research Lab,
Stennis Space Center, MS, USA

K. T. Holland
e-mail: todd.holland@nrlssc.navy.mil

R. A. Holman (✉)
Coastal Imaging Lab, Oregon State University,
Corvallis, OR, USA
e-mail: holman@coas.oregonstate.edu
URL: http://cil-www.coas.oregonstate.edu

1 Introduction

The shallow waters of the littoral zone are the focus of both increasing population pressure and increasing hazards from storms and sea level rise. They are often strategically important and can be hubs for recreation and resource extraction. Living near this dynamic domain requires knowledge of the expected bathymetry and hydrodynamic conditions that will be encountered. In the shallow waters of the surf zone and nearshore domains (commonly defined by depths less than 10 m), these conditions change rapidly. Order one changes in surf zone depths can occur on the storm time scale, rip current channels can form or evolve, and strong currents can appear or disappear with changing offshore waves or even with changing depths through the tidal cycle. As a consequence, climatological information is

of little value in this dynamic region, and predictions must be updated immediately before any important activity.

In the USA, the responsibility for clandestine nearshore characterization for military operations traditionally fell to Navy SEALs and was considered an unpopular and dangerous mission. As a consequence, there has been considerable investment in developing alternate, safer, and simpler methods that avoid the need for a direct presence in denied regions. Similarly, for civilian applications such as coastal zone management, extended measurements are impossible for both economic and logistic reasons, so low cost methods of measuring littoral conditions are clearly needed.

The greatest challenge is estimating the current bathymetry. Given accurate bathymetry and a reasonable approximation of offshore wave conditions from models like Wave Watch III, good predictions of hydrodynamic conditions in the nearshore have been produced by a number of standard models (e.g., Feddersen and Guza 2003; Ruessink et al. 2003). But the development of cheaper or clandestine methods for determining bathymetry has been difficult and the subject of an extended (intermittent) research effort since World War II.

A number of remote sensing approaches have been developed that are based on the measurement of depth-dependent signatures by overhead sensors. In this paper, we will consider one such approach, bathymetry estimation derived from measurements of wave celerity. We will omit discussion of active systems like LIDAR or passive multi- or hyper-spectral methods—not because they are less effective, but because we seek approaches with limited logistical requirements that might be applied to small airborne platforms like the Raven (AeroVironment, Inc), since these are operationally available and not subject to the resource competition of larger observing systems. Celerity-based methods also place no requirement on water visibility or on knowledge of water optical properties, so are useable in turbid waters and to depths that depend only on the wave period but not on the water clarity.

Our objective in this paper is to investigate the issues associated with applying celerity-based bathymetry estimation methods to time-series imagery collected from small unmanned airborne systems (SUASs, also commonly known as Unmanned Aerial Vehicles, or UAVs). In Section 2, we will describe the method and prior demonstrations of performance using either fixed cameras or manned aircraft with sophisticated navigation systems. This will lead to a series of issues that must be addressed associated with the limitations of SUAS data. In Section 3, we will address these problems using a test surrogate of fixed platform data that have been deliberately degraded to mimic the known data problems of SUAS systems. We will then apply the methods to two available SUAS datasets for which ground truth data were available. Finally, we will discuss remaining issues and summarize results.

2 Celerity-based bathymetry estimation

The foundation of this method is the wave dispersion relationship that relates the radial frequency of a wave, σ, to its wavenumber, k,

$$\sigma^2 = gk\tanh(kh) \tag{1}$$

where σ is 2π divided by the wave period, T, and k is 2π divided by the wavelength, L, g is the acceleration due to gravity, and h is the depth (e.g., Dean and Dalrymple 1991). Doppler corrections due to currents are well understood but will be omitted for simplicity.

Typically, the dispersion relationship is used to predict the wavelength of waves of a known period in a known depth of water. However, if both wavelength and wave period can be measured (e.g., by remote sensing), the relationship can be solved numerically to instead find the depth of water. This connection to depth is through a hyperbolic tangent function, tanh, of the ratio of depth to wavelength. In very shallow water (depths less than $L/20$), this sensitivity is somewhat unfavorable to bathymetry estimation in that a fractional error in L yields twice that fractional error in h. The dependence worsens in deeper water as the wavelength approaches a deepwater value ($gT^2/2\pi$) with no further sensitivity to depth. However, Stockdon and Holman (2000) show that wavelengths up to 90% of this value yield reasonable answers. Similarly, while Eq. 1 is strictly valid only for waves of infinitesimal amplitude, Holland (Holland 2001) used excellent in situ measurements to show that outside the surf zone (but shallower than the Stockdon and Holman limit), depth estimates from the linear dispersion relationship were accurate to within 6%.

Early investigations sought to manually estimate L and T from a small set of air photos but found the method to be very noisy for the non-idealized complex wave trains of natural beaches (Williams 1947), especially in light of the above dispersion sensitivity. Thus, the bulk of the intervening research has focused on the development of methods that are statistically robust and recognize the spectral nature of natural incident wave fields (for a good summary, see Plant et al. 2008). We will follow the Plant et al. method, as also recently described by (Holland et al. 2010).

The input data for this analysis are a suite of pixel intensity time series, $I(x_i, y_i, t)$, collected over a dwell, T_d, at a set of discrete locations, $[x_i, y_i]$, where x is the offshore and y the alongshore coordinate. Commonly, these locations correspond to the ground location of every pixel in images

or a regular, interpolated spacing of comparable density. However, spatial coverage is sufficient even with only a few (5–10) pixels per wavelength, and the analysis usually works equally well based on time series from only 0.1% to 1% of the available pixels, provided they are appropriately spaced.

In earlier methods (e.g., Dugan et al. 2001), the analysis was based on the three-dimensional Fourier transform of the data, yielding the variance distribution as a function of frequency and the two vector components of wavenumber, k_x and k_y, that could be fit to Eq. 1 to find a best estimate of depth. However, the basic resolution of standard Fourier transforms depends on the length of the record, so analysis domains were required to span at least a few wavelengths of the observed ocean waves, reducing the spatial resolution of the method. In contrast, in the current method (called cBathy), the Fourier transform is only in the time domain, allowing the frequency partitioning needed to focus the analysis on gravity waves. Wavenumber is then estimated by fitting the spatial patterns of Fourier phase to a model consisting of a single progressive ocean wave for each frequency. For such a case, the normalized cross-spectrum, C_{ij}, between any pair of pixels separated by Δx_{ij} and Δy_{ij} is given by

$$\widehat{C}_{ij} = \exp\left[i\left(k_x \Delta x_{ij} + k_y \Delta y_{ij}\right)\right] \tag{2}$$

Given N pixel locations, the roughly N^2-associated cross-spectra can be fit to determine the wavenumber components for each frequency. This information is then passed to a final depth solver that finds a weighted least squares fit depth to the frequency–wavenumber pairs using Eq. 1. Weighting is by spectral band energy within a frequency range of interest. Other details of the method including methods for computing confidence intervals are described in Holland et al. (2010).

The algorithm was originally developed and tested on an Argus camera system mounted on a fixed tower at the Field Research Facility (FRF) at Duck, North Carolina. Argus stations for making nearshore observations have been developed over several decades, are described by Holman and Stanley (2007), and have the advantage of unlimited dwell (within daylight hours) and fixed pointing geometry. Figure 1 shows an example cBathy result from January 14, 2010, comparing the surveyed bathymetry on the left with cBathy estimates on the right for a 500× 1,000-m beach area. Excluding regions where true depths are less than 0.25 m and a central region for y=400–600 m where a pier contaminates the optical results, the mean and standard deviation of differences between the two data sets are 0.09 and 0.62 m, respectively. Errors are small except over the bar crest region (red) where finite amplitude effects cause some bias and the sharpness of the bar is reduced by smoothing inherent in the analysis algorithm.

The results in Fig. 1 were based on records that were 17 min long (1,024 s), allowing good resolution of the incident wave frequencies and a cross-spectral weighting by

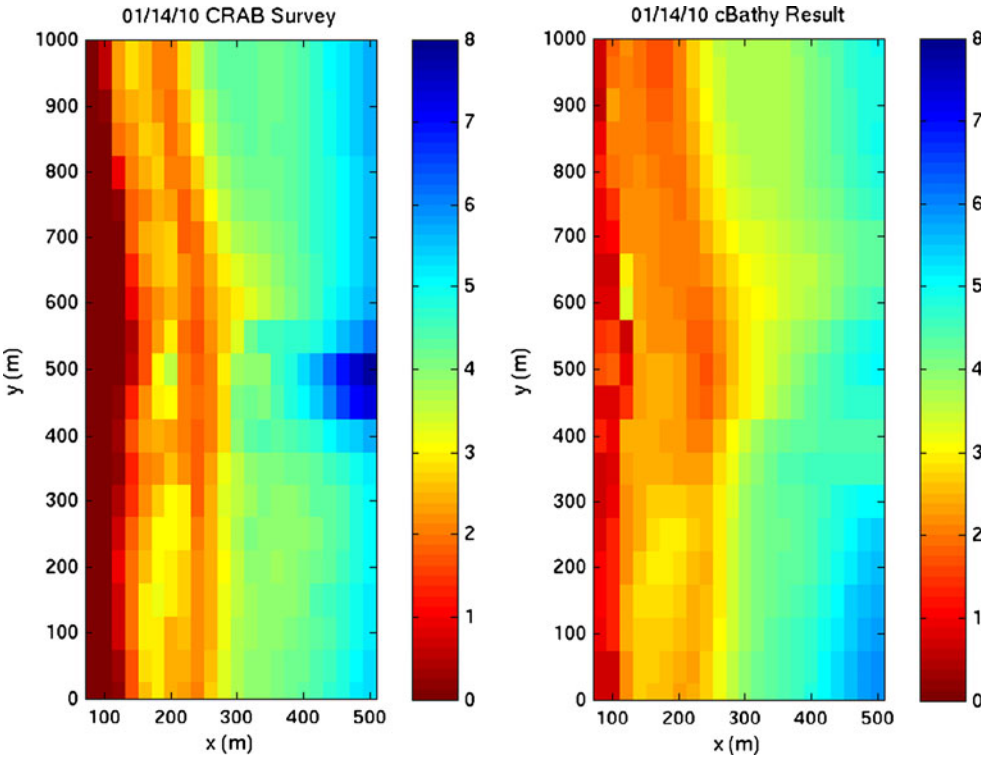

Fig. 1 Comparison of bathymetries collected using an accurate survey system (*left*; estimated 95% error ±5 cm) and that estimated using the cBathy algorithm (*right*). All *scales* are in meters, with the shoreline on the *left*. The nearshore sand bar (*red band*) is well rendered in the cBathy results. Excluding true depths less than 0.25 m and a contaminated region from 400–600 m where a pier interrupts the optical view, the cBathy method had a bias and standard deviation error of 0.098 and 0.62 m, respectively

coherence-squared. Pixel data were sub-sampled to an x and y spacing of 5 and 10 m, respectively, while cBathy results were resolved at x and y spacings of 20 and 50 m, respectively, but were smoothed with a smoothing scale of 40 and 100 m, respectively. Finally, because hourly estimates were available, they could be combined using a Kalman filter to build a robust product over 2 days of collection.

3 Limitations of SUAS data

When the same method is applied to SUAS data, several limitations must be overcome:

a. Record lengths will be short.
b. Records will commonly have gaps, incompatible with normal Fourier analysis.
c. Camera gain can often change significantly, depending on the mix of observed brightness's in the field of view.
d. Image geometries are often inconsistent with filtered navigation data from the UAV.

Of these, the variability of camera gain is the easiest to deal with. Gain changes will introduce low frequency variations in observed signals as the imagery brightens and darkens. Upon Fourier transform, some of this energy will leak into incident frequencies, contaminating the wave content and biasing the analysis. We found that removal of the time-varying array mean intensity from each sample was adequate to remove this contamination. In the following, we discuss the severity and fixes for each of the remaining three problems. The following discussion is based on data from fixed camera sites that have purposely been degraded to mimic problems anticipated from airborne sources.

3.1 Short record limitations

The frequency resolution, Δf, of Fourier analysis is determined by the temporal dwell as $\Delta f = 1/T_d$. For the 1,024-s data runs at the FRF, the incident wave band was well resolved ($\Delta f \sim 0.001$ Hz), and coherence could be computed over a number of plausible incident wave frequency bands. The analysis could then be weighted

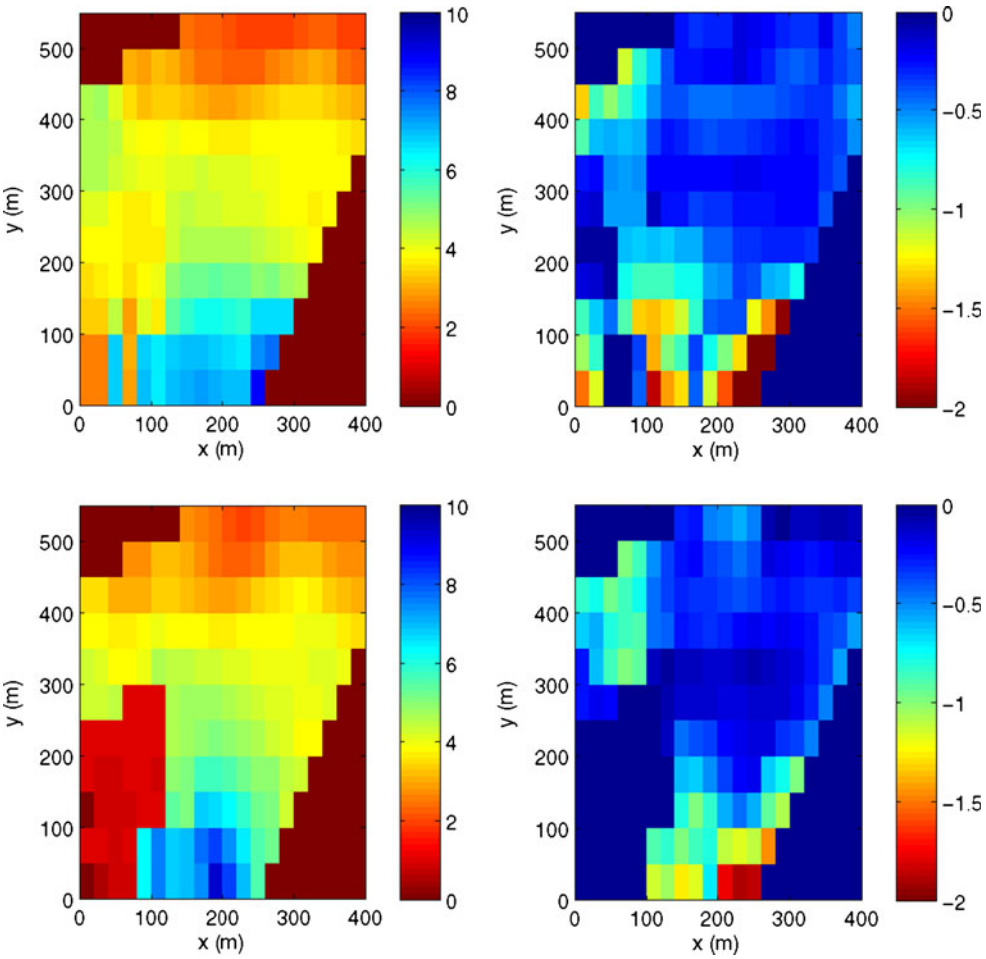

Fig. 2 Comparison of cBathy bathymetry results for a run with 512-s dwell (*upper*) and that computed from just the first 50 s (*lower*). Offshore is to the *bottom of the figure*. Data are from a tower-mounted camera at Santa Rosa Island, Florida on April 17, 2009, 1700 GMT. *Left panels* show the bathymetry; *right panels* show confidence estimates. Depths are in meters

toward the most coherent signals. However, for a SUAS, it is difficult or impractical to maintain dwell on a target for more than about 1 min. Because we no longer have enough frequencies to band average, spectral estimates are noisier, and we can no longer use coherence as a weighting for signal quality.

The tradeoff between dwell and bathymetry error has been investigated by previous authors (Holland et al. 2010; Piotrowski and Dugan 2002). Holland et al. (2010) developed a simulation tool and found that record lengths of 50 s were theoretically sufficient to yield useful bathymetry (with relative depth errors of less than 20%). Figure 2 shows an example comparison of bathymetry results from a 512-s data run from a fixed camera mounted on a 100-m-tall tower at Eglin Air Force Base (AFB), and the bathymetry computed based only on the first 50 s. The similarity is striking and supports the result of Holland et al.

In general, the 50-s limitation is too long to be accommodated by simple fly-by sampling with a fixed look camera but can instead be achieved in several ways. The data collections discussed below were based on a fixed forward-look camera sampled while the SUAS flew in a slowly descending trajectory, staring at a surf zone target point. Alternately, a circular orbit can be used to achieve dwell using a side-look fixed camera. A preferable solution would be a programmed stare using a gimbaled camera; however, no such data collections were available for testing during this study.

3.2 The record gap problem

The ground (sea?) footprint of each overhead image covers a region that varies from frame to frame with the changing camera location and aim. Likely there will be a small region with continuous coverage, but this will be a small fraction of the size of the region for which there is substantial, but discontinuous, coverage. Figure 3 shows the spatial map of percent temporal coverage for an example slow-descent acquisition sequence, a trajectory chosen to maximize stability of coverage. Even for the case, the region of continuous coverage is much smaller than the region of substantial coverage, so we require a Fourier transform method that allows record gaps.

Fourier transforms are found using the equation

$$Y(f) = \sum_{n=1}^{N} y(t_n) \exp(-i(2\pi f t_n)) \tag{3}$$

where y is the time series signal and Y its frequency-dependent Fourier transform. If the time series are continuous and equally spaced, Fast Fourier transform (FFT) methods may be used. However, even if the time series have gaps, Eq. 3 can still be used for the existing

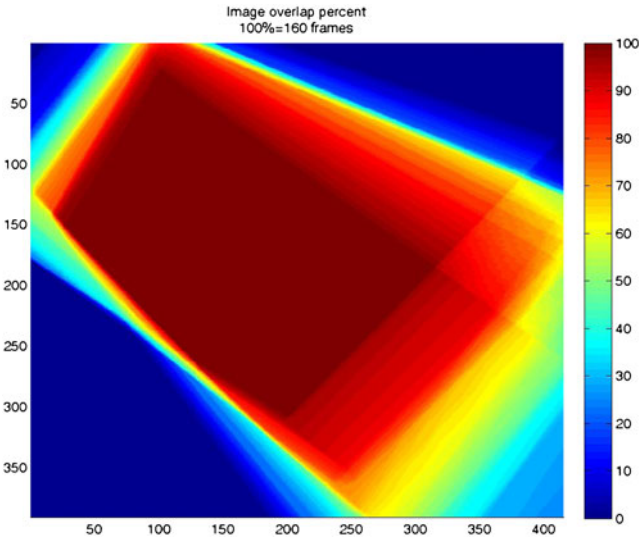

Fig. 3 Percent temporal coverage for example data for a descending stare collection. Even with this intentionally stable sampling method, the region of continuous coverage is much smaller than the region of substantial coverage

data. The gaps violate assumptions about orthogonality, and the resulting Fourier transforms will be only approximations. To test this, approach, non-gappy data from a tower-mounted camera were degraded by the addition of gap patterns found for an actual SUAS flight (Fig. 3) and the approximate Fourier transform computed. When the corresponding approximate time series was found by inverse FFT and compared to the original (non-gappy) time series, it was found that wave signal was visually well approximated even for records with gaps of up to 50% of the dwell. Similarly, spatial maps of wave phase (derived from the complex Fourier transform, $Y(f)$ and the primary input to the cBathy analysis) were very well approximated even for 50% gappy data, and cBathy results were very similar for gappy and continuous time series.

Thus, there are two keys to improve performance of bathymetry extraction methods for SUAV data. First, relaxation of the criterion of continuous sampling greatly improves the effective sampling area available from SUAS data and is essentially a requirement for success in this method. Second, the replacement of spatial Fourier methods for finding wavenumber by the wave phase fitting of cBathy (Eq. 3) allows discontinuous and short spatial sampling to be used, again greatly expanding the utility of otherwise imperfect data.

3.3 Image navigation accuracy

The analysis methods of cBathy are based on time series data from fixed, known locations. However, the projected

world location associated with any pixel depends on the changing camera location and pointing angles through known photogrammetric relationships (Holland et al. 1997). These data are transmitted from the SUAS in real time and, in principle, allow accurate ground projection of each frame.

Pennucci et al. (2008) studied the accuracy of the downlinked onboard navigation data for a Raven B SUAS for the application of ground plane mapping of a suite of observed ground targets whose locations were known. They found that errors of 50 m were typical for SUAS altitudes of ~300 m and that these errors would swamp an analysis like cBathy unless corrected using fixed ground control features in the image. The specific location of these features is less important than the fact that they are fixed and allow stabilization of imagery for which high frequency aim point changes are not accurately reflected in filtered navigation metadata. Thus, the analyses described below were based on imagery for which shoreline features were visible and used for stabilization.

The requirement for partial shoreline visibility in each frame is a restrictive complication for the operation use of these methods. Possible solutions being investigated include the use of gimbaled motion-compensating camera systems and the potential for inverse solutions for pointing angle errors based solely on image (moving) ocean waves, both discussed further below.

4 Example bathymetry results

Performance is ultimately judged by the ability to produce bathymetry from actual SUAS data files. We present two cases, one from Santa Rosa Island on the Florida panhandle and the second from Silver Strand Beach in Southern California.

The Santa Rosa data run was 54-s long, sampled at 6 Hz and flown from onshore to offshore in a slowly descending stare at roughly 5-s incoming waves. High frequency variations in image view angles were corrected using fixed ground control features in the lower portion of the frame. Figure 4 shows the resulting cBathy estimate of bathymetry (upper panel) and the associated 95% confidence intervals on those estimates (lower panel). Analysis spanned a 320 (x) by 240 (y) region with resolution of 20 m in either direction. The bathymetry is seen to deepen plausibly to the south (Gulf of Mexico). Excluding a 60-m wide region on the east boundary of this analysis box (not shown) that was objectively identified by the error bars as having poor performance, the mean confidence was 0.25 m.

Figure 5 compares these bathymetry estimates with a GPS ground truth survey carried out from 23 to 28 January 2009, in support of this effort. Survey data were reduced to an assumed local geoid representative of mean sea level, but actual tide level was neither known nor corrected for. Errors in geoid and tide presumably contributed to the

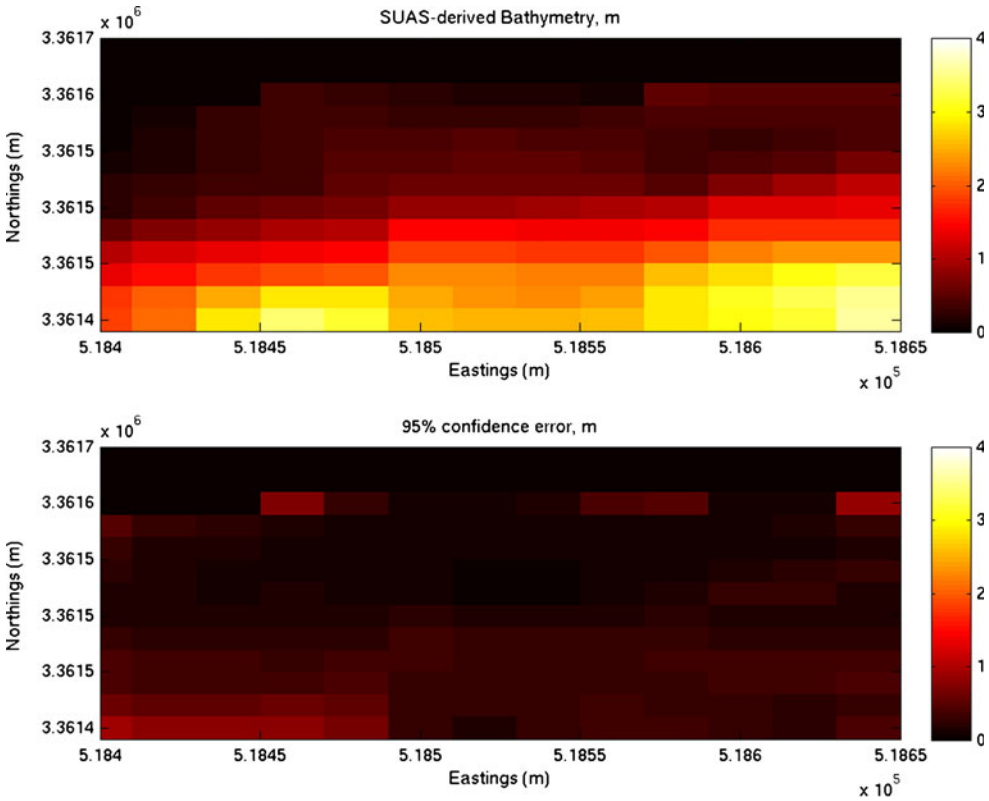

Fig. 4 Estimated bathymetry from Santa Rosa for January 27, 2009, 1413 CST (*upper panel*) and associated confidence limits (*lower panel*). The deep water of the Gulf of Mexico is to the *south*. Estimates span a 320 (x) by 240 (y) region

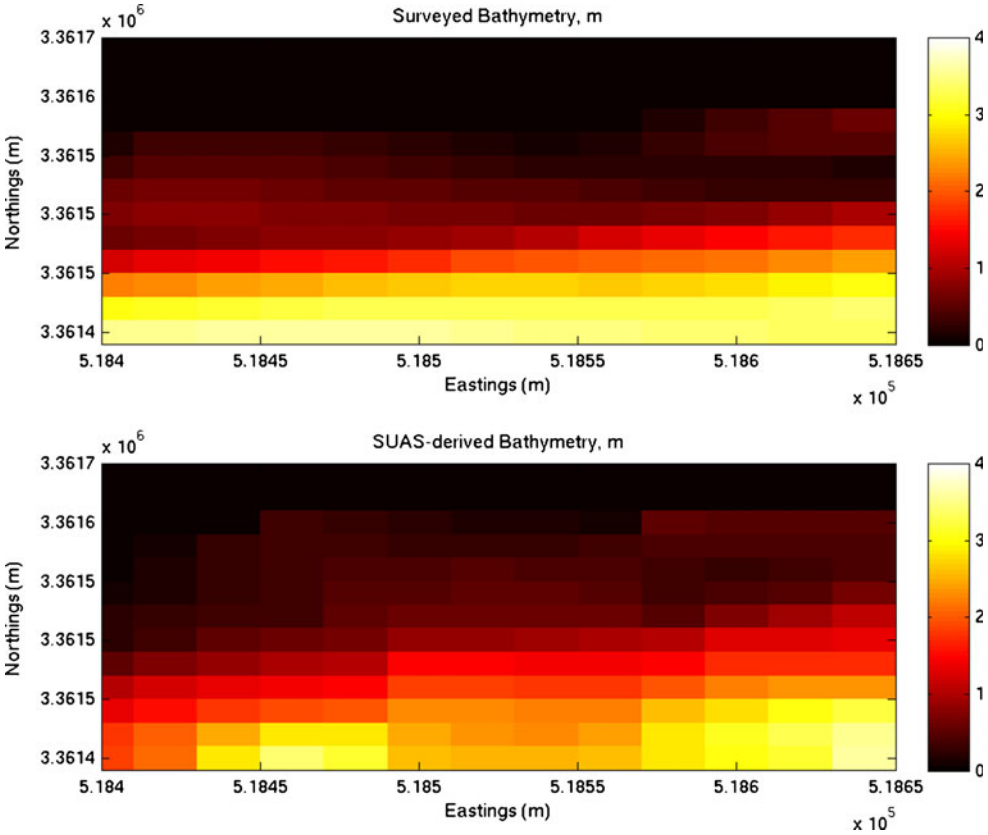

Fig. 5 Comparison of ground truth bathymetry found using coupled GPS–fathometer survey methods (*upper panel*) with cBathy-estimated bathymetry from a 54-s-long SUAS data collection (*lower panel*). The standard deviation of the differences was 0.55 m (R^2=0.87)

observed 1.06-m bias in irrecoverable ways. After bias removal, the standard deviation of the differences was 0.51 m. Survey and cBathy results were highly correlated (R^2=0.87). To determine depth sensitivity of performance, calculations were carried out for 1-m-depth bins. For mean depths in each bin of 0.5, 1.5, 2.5, and 3.5, the standard deviations were 0.26, 0.41, 0.29, and 0.55 m respectively. Note that all statistics were computed as weighted averages, weighted by the inverse of the cBathy error estimate.

Data were also collected at Silver Strand Beach on December 9, 2009, and compared to a GPS survey collected from 4 to 7 December. Two SUAS data collections were analyzed, and the results merged in a weighted average, where the weighting was taken as the inverse on the confidence intervals for each estimate. Again, a bias associated with unmeasured tide and geoid issues was removed. Figure 6 compares the retrieved bathymetry (right panel) with the GPS survey data (left

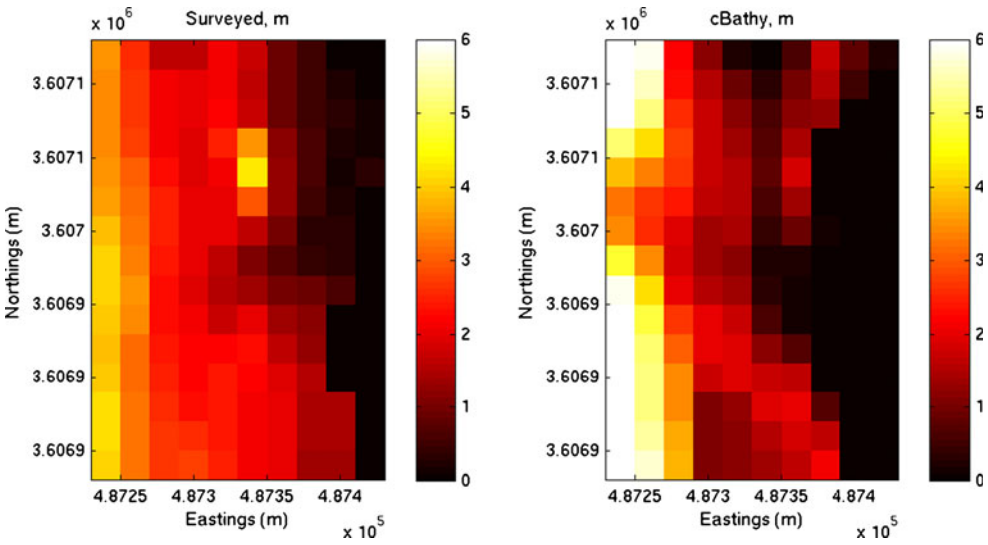

Fig. 6 Comparison of bathymetry retrieved using the cBathy analysis of SUAS data (*right panel*) and a ground truth GPS survey (*left panel*) for data collections December 9, 2009 at Coronado Beach, California. Deeper waters of the Pacific Ocean are to the *left*, the dry beach to the *right*. Intermediate depths are well measured, but a deep bias offshore causes a total error standard deviation of 1.45 m. Of estimates, 73% are within 1 m of the surveyed values

panel). The analysis area spanned 180×240 m in the across-shore and alongshore directions, respectively, with a spatial resolution of 20 m.

The shape and contours of the beach are well estimated by the cBathy analysis and show a 100-m-wide terrace bounded by a steep seaward drop-off. The largest discrepancies are offshore, where cBathy over-estimates depths for true depths greater than about 4 m. For true depths between 0.5 and 3.5 m, the standard deviation of the match was 1.19 m. However, 73% of the estimates were within 1 m of the true depth, and the best estimates are for depths from 2 to 3 m. These results seem particularly good given the short (30.5 s) length of the data collection.

5 Discussion

The example results shown above demonstrate that airborne sampling and bathymetry estimation can be successfully carried out on a small unmanned system such as are commonly used in operational areas. Sufficient dwell can be achieved using simple flight patterns such as a straight descending stare or a circular orbit. The increasing availability of gimbaled systems will simplify the collection process in two ways, both allowing more flexible fight patterns while maintaining dwell and reducing gappiness associated with occasional look-away for fixed aim cameras on a slightly unstable moving platform.

Image navigation remains a primary concern. Downlinked airframe orientation data (pitch, roll, yaw) are filtered on board to improve autopilot stability, and thus do not capture the high-frequency turbulent shifts of normal flight that will shift the aim point of snapshots. For the above analyses, tracking land-based control points compensated for this noise, but this requires that some small fraction of the image always includes land. Methods based only on the imaged wave field are usually assumed invalid since the waves are not fixed, but instead move at a spatially non-uniform way depending on depth. However, this approach should not be dismissed prematurely. If the predominant source of error is assumed to be the camera pointing angles (i.e., GPS position errors are considered negligible by comparison), then error in each pointing angle will yield a predictable and unique distortion of the imaged wave field. For example, for a forward-looking camera, a pitch error might increase magnification in the distance while shrinking nearby features, whereas a roll error would magnify features on one side of the image while shrinking the other side. It may be possible to exploit the orthogonal nature of the imaged wave field distortion to solve for the inevitable high frequency errors in pointing angles and provide a consistent solution for water-based image stabilization. This could be a very rewarding future research problem.

Progress on this project was slowed by the difficulty of obtaining usable wave imagery at domestic test sites. One issue was the current US policy confusion over dealing with UAVs in US air space, an issue that will likely be addressed in the next decade and would not be a problem in offensive (or defensive) foreign operations. We were also stymied at times by placid ocean conditions (in association with optimal flight conditions) with no discernable wave activity. Again, this issue will be site-dependent, and low wave sites may also be more amenable to complementary bathymetry estimation methods such as multi/hyper-spectral approaches.

6 Conclusions

Methods to estimate nearshore bathymetry based on observations of depth-dependent wave celerity have been investigated previously but never for SUASs. In this paper, we have investigated the issues associated with applying existing methods to SUAS data, developed methods to mitigate limitations, and tested the resulting algorithms at two different ocean sites.

The primary concerns for SUAS applications are (a) short record lengths, (b) gaps in time series records, and (c) unavoidable errors in image navigation. Prior work had recommended a minimum of 50-s record length for bathymetry estimation purposes (Holland et al. 2010) and suggested optimum flight patterns. Reasonable results were achieved here with 54- and 31-s record lengths. It was found that record gaps, an inevitable consequence of imperfect and unsteady camera aiming during flight, could be readily handled using a full Fourier Transform (not Fast Fourier Transform) computation over available gappy data provided that data coverage included at least 50% of the record. Finally, image navigation issues, currently the main limitation to SUAS analyses, could be stabilized using shore-based fixed control points now and, potentially, wave only analyses in the future.

Two SUAS data collection tests demonstrated success of this method. For a 54-s data run at Santa Rosa Island, the standard deviation of errors (compared to in situ survey data) was 0.55 m. For a similar but short (30.5 s) west coast data run, the shape of the beach was replicated, but errors were larger (standard deviation of 1.9 m). However, 73% of the data were within 1 m of being correct, and errors were concentrated offshore.

Acknowledgments This work was supported by the Office of Naval Research through funding of the rapid transition project "Estimation of surf zone bathymetry using Unmanned Aircraft Systems" (PE no. 0602435).

References

Dean RG, Dalrymple RA (1991) *Wave wave mechanics for engineers and scientists*, 353 pp., World Scientific Publishing, Cornell

Dugan JP, Piotrowski CC, Williams JZ (2001) Water depth and surface current retrievals from airborne optical measurements of surface gravity wave dispersion. J Geophys Res 106(C8):16903–16915

Feddersen F, Guza RT (2003) Observations of nearshore circulation: alongshore uniformity. J Geophys Res 108(C1):3006

Holland KT (2001) Application of the linear dispersion relation with respect to depth inversion and remotely sensed imagery. IEEE Trans Geosci Remote Sens 39(9):2060–2072

Holland KT, Holman RA, Lippmann TC, Stanley J, Plant N (1997) Practical use of video imagery in nearshore oceanographic field studies. IEEE J Ocean Eng 22(1)

Holland KT, Lalejini DM, Spansel SD, Holman RA (2010) Littoral environmental reconnaissance using tactical imagery from unmanned aircraft systems, paper presented at SPIE Defense Security and Sensing Conference, SPIE, Orlando

Holman RA, Stanley J (2007) The history and technical capabilities of Argus. Coast Eng 54:477–491

Pennucci G, Conley DC, Holman RA (2008) Quantitative image analysis for maritime missions using an autonomous distributed sensor system, in *Fusion 2008*, edited, p. paper #256907519, Cologne.

Piotrowski CC, Dugan JP (2002) Accuracy of bathymetry and current retrievals from airborne optical time-series imaging of shoaling waves. IEEE Trans Geosci Remote Sens 40(12):2602–2612

Plant NG, Holland KT, Haller M (2008) Ocean wavenumber estimation from wave-resolving time series imagery. IEEE Trans Geosci Remote Sens 46:2644–2658

Ruessink BG, Walstra DJR, Southgate HN (2003) Calibration and verification of a parametric wave model on barred beaches. Coast Eng 48:139–149

Stockdon HF, Holman RA (2000) Estimation of wave phase speed and nearshore bathymetry from video imagery. J Geophys Res 105 (C9):22,015–022,033

Williams WW (1947) The determination of gradients on enemy-held beaches. Geogr J 109(1–3):76–93